[CANCER RESEARCH 64, 1315–1322, February 15, 2004]

# Enhanced Tumor Formation in Cyclin D1 × Transforming Growth Factor β1 Double Transgenic Mice with Characterization by Magnetic Resonance Imaging

**Natasha G. Deane,[1,2] Haakil Lee,[2] Jalal Hamaamen,[1] Anna Ruley,[1] M. Kay Washington,[3] Bonnie LaFleur,[5] Snorri S. Thorgeirsson,[4] Ronald Price,[2] and R. Daniel Beauchamp[1,6]**

*Departments of [1]Surgery, Division of Surgical Oncology, [2]Radiology, Division of Radiological Sciences, and [3]Pathology, Vanderbilt University Medical Center, Nashville, Tennessee, [4]Laboratories of Experimental Carcinogenesis and Chemoprevention, Division of Cancer Etiology, National Cancer Institute, Bethesda, Maryland, and Departments of [5]Preventative Medicine and Biostatistics and [6]Cell & Developmental Biology and Cancer Biology, Vanderbilt University Medical Center and the Vanderbilt-Ingram Cancer Center, Nashville, Tennessee*

## ABSTRACT

**Transgenic mice that overexpress cyclin D1 protein in the liver develop liver carcinomas with high penetrance. Transforming growth factor β (TGF-β) serves as either an epithelial cell growth inhibitor or a tumor promoter, depending on the cellular context. We interbred LFABP-cyclin D1 and Alb-TGF-β1 transgenic mice to produce cyclin D1/TGF-β1 double transgenic mice and followed the development of liver tumors over time, characterizing cellular and molecular changes, tumor incidence, tumor burden, and tumor physiology noninvasively by magnetic resonance imaging. Compared with age-matched LFABP-cyclin D1 single transgenic littermates, cyclin D1/TGF-β1 mice exhibited a significant increase in tumor incidence. Tumor multiplicity, tumor burden, and tumor heterogeneity were higher in cyclin D1/TGF-β1 mice compared with single transgenic littermates. Characteristics of cyclin D1/TGF-β1 livers correlated with a marked induction of the peripheral periductal oval cell/stem cell compartment of the liver. A number of cancerous lesions from cyclin D1/TGF-β1 mice exhibited unique features such as ductal plate malformations and hemorrhagic nodules. Some lesions were contiguous with the severely diseased background liver and, in some cases, replaced the normal architecture of the entire organ. Cyclin D1/TGF-β1 lesions, in particular, were associated with malignant features such as areas of vascular invasion by hepatocytes and heterogeneous hyperintensity of signal on T2-weighted magnetic resonance imaging. These findings demonstrate that TGF-β1 promotes stem cell activation and tumor progression in the context of cyclin D1 overexpression in the liver.**

## INTRODUCTION

Hepatocellular carcinoma (HCC) is one of the most prevalent and intractable of cancers, causing as many as half a million deaths per year worldwide. Although the incidence of HCC historically has been significantly higher in Asia than in the western hemisphere, this difference has been attributed to the time exposure of the respective populations to the hepatitis C virus (1). With the spread of hepatitis C to western Europe and North and South America during recent decades, the incidence of the disease is expected to increase dramatically worldwide, making this an even more significant problem in cancer research for western society in the years to come (2). A number of genetic variants of HCC have been characterized (3). Among these, more aggressive forms have been associated with increased expression of Cyclin D1 (4, 5).

Cyclin D1 is a key cell cycle regulatory protein and a known oncogene (6). Cyclin D1 expression is required for passage of replicating cells through the $G_1$ cell cycle checkpoint, and cyclin D1 up-regulation is associated with hepatocellular replication following partial hepatectomy in mice and rats (7). Constitutive cyclin D1 expression *in vitro* causes fibroblasts to exhibit a shortened transit time into the cell cycle, reduced cell size, reduced dependency on serum growth factors, and an acquired ability to grow colonies in soft agar (8–10). Constitutive overexpression of cyclin D1 in the liver of transgenic mice *in vivo* leads to the development of hepatocellular adenomas and HCCs with high penetrance (11).

Transforming growth factor β (TGF-β, including types 1, 2, and 3) is a potent inhibitor of epithelial cell proliferation. The growth-inhibitory activity of TGF-β is implicated in the regulation of hepatocellular apoptosis and growth inhibition following tissue injury and regeneration (12). The growth-inhibitory effects of TGF-β are modulated through the type II receptor and the Smad-dependent signaling pathway (13). Escape from or resistance to the growth-inhibitory effects of TGF-β is an important event in multistep carcinogenesis (13, 14). Studies in cell culture suggest that overexpression of cyclin D1 can bypass the $G_1$ cell cycle arrest induced by TGF-β (15). TGF-β production by dysplastic hepatocytes in experimental precancerous mouse livers represents a protective mechanism for the inhibition of excessive cellular proliferation but also causes selective pressure on cells to become resistant to the growth-inhibitory effects of TGF-β (16). Known tumor-promoting effects of TGF-β, including enhancement of extracellular matrix deposition, degradation angiogenesis (13, 17), and conversion of transformed epithelial cells to a more invasive mesenchymal phenotype (*e.g.*, EMT), are preserved when growth-inhibitory responses are lost (18) and may in turn enhance tumor development. Importantly, elevated TGF-β levels also are associated with clinical examples of HCC (19, 20).

We hypothesized that the known tumor-suppressive effect of TGF-β is overcome by constitutive cyclin D1 overexpression in the LFABP-cyclin D1 mouse model, whereas known tumor-promoting effects of TGF-β remain intact. Previous mouse models using TGF-β overexpression have provided mixed results in this regard, depending on the tissue and the molecular context of the transgene. In mammary glands and keratinocytes, TGF-β overexpression confers resistance to tumor formation by oncogenes and carcinogens (18, 21–23), whereas in livers, TGF-β overexpression confers enhanced tumor susceptibility (24). We were interested to determine whether the growth-inhibitory or tumor-promoting effects of TGF-β1 would predominate in the molecular context of LFABP-cyclin D1 transgenic livers. We interbred the Alb-TGF-β1 transgenic and the LFABP-cyclin D1 transgenic mouse lines to create cyclin D1/TGF-β1 single transgenic and wild-type age-matched littermates and performed an analysis of tumor growth in the offspring.

Finally, we introduced the use of magnetic resonance imaging (MRI) to follow tumor development noninvasively and to aid in the characterization of tumor malignancy. MRI is a powerful imaging modality for detecting and characterizing deep soft tissue cancers. Although not favored clinically for the detection of metastatic disease

Received 6/16/03; revised 12/8/03; accepted 12/15/03.

**Grant support:** NIH grants DK52334 and CA69457 (R. D. Beauchamp) and Vanderbilt-Ingram Cancer Center Support grant 5P30CA68485. N. G. Deane is supported by an NIH Multidisciplinary Research Training Grant in Cancer Imaging (CA92043).

The costs of publication of this article were defrayed in part by the payment of page charges. This article must therefore be hereby marked *advertisement* in accordance with 18 U.S.C. Section 1734 solely to indicate this fact.

**Requests for reprints:** Natasha Deane, D2300, Medical Center North, Vanderbilt University Medical Center, 1161 21st Avenue South, Nashville, Tennessee 37232-2730.

to the liver over ultrasound and computed tomography, MRI compares favorably with ultrasound, computed tomography, and positron emission tomography and has emerged as the imaging modality of choice for primary HCC (25, 26). Advantages of this modality include the ability of MRI to aid in the assessment of tumor malignancy by identifying fatty degeneration, vascular invasion, and peritumoral edema. Particularly useful for the characterization of primary malignancies in the liver has been T2-weighted MRI, which produces significantly higher mean contrast between malignant HCC and normal liver (27–29). We used MRI to image tumor incidence and growth rate and to ascertain malignancy in the LFABP-cyclin D1 and cyclin D1/TGF-$\beta$1 mouse models of HCC, thereby introducing a mechanism for decreasing the number of animals required for a long-term study such as this one without sacrificing characterization.

## MATERIALS AND METHODS

**Mice.** Male B6CBA Alb-TGF-$\beta$1 transgenic mice were mated with female C57BL6 LFABP-cyclin D1 transgenic mice, and offspring were typed for the presence of each transgene. Wild-type, LFABP-cyclin D1, and Alb-TGF-$\beta$1 single transgenic mice were maintained as controls along with experimental cyclin D1/TGF-$\beta$1 transgenic offspring according to the National Research Council Committee on Care of Laboratory Animal Resources Commission on Life Sciences' *Guide for the Care and Use of Laboratory Animals* with Institutional Animal Care and Use Committee approval. Animals were housed in the Vanderbilt University Medical Center vivarium (accredited by the American Association for Accreditation of Laboratory Animal Care).

DNA was collected from fragments of ear flap tissue for genotype analysis. PCR for the LFABP-cyclin D1 and Alb-TGF-$\beta$1 transgenes was performed as reported previously (11, 24).

**Pathology and Histology.** Age-matched BL6CBA F1 littermates from Alb-TGF-$\beta$1 and LFABP-cyclin D1 crosses representing wild-type, single transgenic control and cyclin D1/TGF-$\beta$1 experimental animals were maintained in a pathogen-free environment for up to 17 months of age. At 6 months of age and again at 12 months of age, separate cohorts of wild-type, single transgenic and double transgenic animals ($n \geq 4$ each) were killed by $CO_2$ asphyxiation and underwent autopsy. Particular attention was addressed to livers, intestines, lungs, and kidneys of these animals. On autopsy, body weights and liver weights were determined, and heparinized blood was collected for the preparation of plasma. The measure of hepatomegaly is expressed as compared with wild type for each transgenic group [(transgenic liver/body weight) − (wild-type liver/body weight)]/(wild-type liver/body weight), and the average measure across the remaining three groups was tested using ANOVA.

Levels of circulating TGF-$\beta$1 were determined using plasma derived from mouse blood collected first at weaning and again at autopsy in a human TGF-$\beta$1 ELISA system (R&D Systems, Minneapolis, MN) that measures activated and latent forms of the protein. Immunostaining paraffin-embedded liver sections for TGF-$\beta$ and CD31 was performed following inactivation of endogenous peroxidase activity using 0.03% hydrogen peroxide and antigen retrieval. Tissue sections were incubated with rabbit antihuman TGF-$\beta$1(v) (Santa Cruz Biotechnology, Inc., Santa Cruz, CA) diluted 1:150 for 30 min or with goat anti-Pecam-1 (Santa Cruz Biotechnology) diluted 1:400 for 45 min. Sections on the same slide without primary antibody treatment served as negative controls. The DakoCytomation (rabbit and goat, respectively; Carpinteria, CA) Envision system, 3,3′-diaminobenzidine/horseradish peroxidase, was used to produce specific visible staining.

Harvested livers were examined carefully on autopsy, and portions were either fixed in 4% paraformaldehyde (routinely the left lobe only) or flash frozen. Fixed tissues were dehydrated and embedded in paraffin. Five-$\mu$m sections from paraffin blocks were placed on charged slides and prepared for staining. H&E and Gomori's one-step trichrome (green) were used for general and component staining.

In blinded analysis of H&E-stained slides, scores reflecting kidney disease and hepatic disease were derived. For kidney lesions, individual scores of 0 = no abnormality (1–2 = degree of periglomerular fibrosis; 1–3 = degree of mesangioproliferation; and 1–3 = degree of glomerular collapse) were added to achieve an overall disease score. Scores for hepatic disease were based on the following features: cytomegaly and nuclear atypia (scored 0–2), distorted hepatic architecture in the form of nodularity (scored as 0 = none; 1 = surrounding central veins only, zone 3; 2 = focally confluent; and 3 = confluent) and presence or absence of proliferation in terminal cells of bile duct epithelium (scored as 0 = quiescent and 1 = proliferation). Comparisons of tumor pathology in LFABP-cyclin D1, cyclin D1/TGF-$\beta$1 mice, and the control groups were made using ANOVA techniques for mean histopathologic score and exact methods (based on an extension of Fisher's exact test statistics for R × C contingency tables) for the individual measurements. The histopathologic score was calculated by summation of the individual scores for cytomegaly, nuclear atypia, proliferation in bile duct epithelium, and nodularity; these individual measurements were rated on a quasi-ordinal scale, with higher scores indicating more changes.

Counts of apoptotic bodies were obtained directly from H&E-stained sections of livers at 6 and 12 months of age by averaging counts of apoptotic bodies counted in 10 high-power (400×) fields of magnification from uniform sections. Hepatocellular proliferation and apoptosis were examined using a Poisson regression analysis on the actual counts of cells showing either mitotic or apoptotic bodies.

By 12 months of age, counts of developing carcinomas were derived by counting lesions in uniform H&E-stained sections. Tumor incidence and multiplicity in LFABP-cyclin D1 and cyclin D1/TGF-$\beta$1 mice were described and tested using confidence intervals (CIs) around the relative risk; this included a stratified analysis by age (two groups: ≤12 months *versus* >12 months). Written descriptives for each tumor lesion detected were provided (by K. W.).

**Immunoprecipitation and Immunoblotting.** Fifty to 100 mg of frozen liver tissue per 3 ml of ice-cold radioimmunoprecipitation assay buffer [1× PBS with 1% Igepal (NP40, Sigma, Co., St. Louis, MO), 0.5% sodium deoxycholate, and 0.1% SDS] with proteinase inhibitors (10 $\mu$l/ml phenylmethylsulfonyl fluoride, 30 $\mu$l/ml of aprotinin, and 10 $\mu$l/ml of 100 nM sodium orthovanadate) were used in the preparation of protein lysates by sonication. Detection of Smad2/3:Smad4 complexes and Smad4 protein was accomplished as described previously (30). Lysates from ≥10 animals of 6–12 months of age from each group were evaluated for Smad4 expression and Smad2/3:Smad4 complex formation. Proportions of animals in each group that scored positively on these measures were reported with 95% CIs.

**Abdominal Imaging.** Beginning at 9 months of age, separate cohorts of LFABP-cyclin D1 and cyclin D1/TGF-$\beta$1 animals ($n > 6$ of each genotype) were followed monthly for the development of liver tumors by MRI. Mice were anesthetized using 1.2% isoflurane in $O_2$ (2 l/min) using a ventilator (Anesco Inc., Georgetown, KY) throughout the imaging process. Body temperature was maintained using circulated warm water (37–39°C) controlled with a thermostat. Individual mice then were placed in a 4.7-T spectroscopy imaging system (Varian, Inc., Palo Alto, CA) magnet and guided by markings on the carrier external to the magnet for precise placement. A saddle coil (9 cm inside diameter) was used as a transmitter and, a surface coil (2.5 cm inside diameter) was used as a receiver. T1-weighted scout images (repetition time/echo time = 800/14 ms) were captured to confirm mouse placement and target location. A 1.8-cm-long region encompassing the liver was imaged from the base of the lung using 18 × 1-mm slices and a 3.5 cm × 3.5-cm field of view. Multislice fat-suppressed T1-weighted spin-echo (repetition time/echo time = 800/14 ms) and T2-weighted (repetition time/echo time = 3000/50 ms) MRIs from the mice were transferred to a Sun Ultra workstation (Sun Microsystems, Inc., Mountain View, CA) and processed. All of the detected areas of interest were followed monthly to determine tumor volume and growth rate characteristics. Analysis of tumor volume was achieved using the image processing software package ImageJ.[7]

**Statistical Analysis.** All of the analyses were performed using SAS, version 8.2 (SAS Institute, Cary, NC).

## RESULTS

Mean circulating levels of TGF-$\beta$1 in Alb-TGF-$\beta$1 and LFABP-cyclin D1 single transgenic lines were elevated above wild-type levels

[7] http://rsbi.info.nih.gov/ij/.

in weanling mice but to a lesser degree than in cyclin D1/TGF-$\beta$1 mice as follows: wild type = 16.9 ± 4.1 ng/ml, Alb-TGF-$\beta$1 = 43 ± 9.2 ng/ml, LFABP-cyclin D1 = 48.6 ± 19.4 ng/ml, and cyclin D1/TGF-$\beta$1 = 63.7 ± 29 ng/ml ($n \geq 4$ in all of the groups). Circulating TGF-$\beta$1 in all of the transgenic groups decreased to wild-type levels by 6 months of age, consistent with earlier, well-documented observations in the parental line, in which transgene expression in the liver remained robust through 12 weeks of age (24). Thus, the levels of circulating TGF-$\beta$1 in the cyclin D1/TGF-$\beta$1 mice were found to be higher than in either of the single transgenic controls, suggesting an additive effect, although mean differences between all of the genotypes were not statistically significant.

As a measure of the pathophysiologic levels of TGF-$\beta$1 deposition in the livers of experimental animals, an immunohistochemical stain for TGF-$\beta$1 was performed. This stain revealed perivenous TGF-$\beta$1 activity in LFABP-cyclin D1 and cyclin D1/TGF-$\beta$1 livers at 6 months of age associated with dysplastic cells (Fig. 1, *A* and *B*). In cyclin D1/TGF-$\beta$1 mice 12 months of age or older, the staining still was strong but was no longer restricted to a distinct zonal pattern as it was in the LFABP-cyclin D1 livers (not shown). TGF-$\beta$1 stain was excluded frequently from some, but not all, nodules forming in the liver (not shown).

Two phenotypic markers emerging from careful study of the parental Alb-TGF-$\beta$1 line, namely hepatic fibrosis and kidney disease, were useful surrogate markers for the levels of circulating active TGF-$\beta$ in experimental mice (24, 31). These characteristics were found to segregate reliably with the Alb-TGF-$\beta$1 transgene and marked the downstream effect of activated TGF-$\beta$1 from the Alb-TGF-$\beta$1 transgene in the animals. Although marked collagen deposition of portal arteries is seen in Alb-TGF-$\beta$1 and cyclin D1/TGF-$\beta$1 livers, no significant deposition is seen in either wild-type or LFABP-cyclin D1 livers (Fig. 1, *C* and *D*). Mean scores for fibrosis at 12 months ($n$ = 2–5) were as follows: wild type = 0 ± 0, LFABP-cyclin D1 = 0.4 ± 0.9, Alb-TGF-$\beta$1 = 3 ± 0, and cyclin D1/TGF-$\beta$1 = 4 ± 0. When scores from LFABP-cyclin D1 and cyclin D1/TGF-$\beta$1 mice were compared, a significant difference in fibrosis between the two groups was found ($P < 0.0001$). Lesions in the kidney that are associated with expression of the Alb-TGF-$\beta$1 transgene consist of a global diffuse increase in glomerular size caused by mesangioproliferation with mesangiopathy, significant collagen deposition, and periglomerular fibrosis; all of the features have been described in detail elsewhere (31). When scores for these features were compared ($n$ = 8 LFABP-cyclin D1 and $n$ = 8 cyclin D1/TGF-$\beta$1), significant differences were seen between LFABP-cyclin D1 control and cyclin D1/TGF-$\beta$1 experimental animals (LFABP-cyclin D1 mean = 1.0 ± 0.38; cyclin D1/TGF-$\beta$1 mean = 4.37 ± 0.65; $P$ = 0.0005).

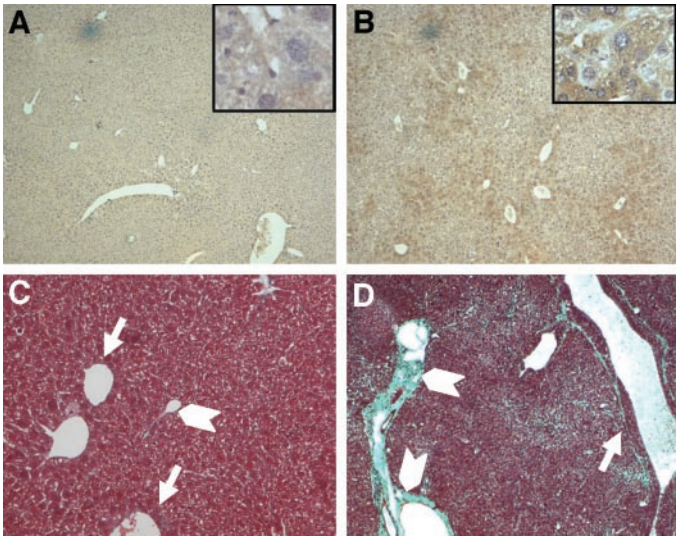


Fig. 1. Cyclin D1/transforming growth factor $\beta$1 (TGF-$\beta$1) livers exhibit high levels of TGF-$\beta$1 expression and are fibrotic. *A,* LFABP-cyclin D1 liver (age 6 months) at 50× magnification shows light background stain for TGF-$\beta$1 and little to no staining in pericentral hepatocytes (inset, 200× magnification). *B,* cyclin D1/TGF-$\beta$1 liver (age 6 months) at 50× magnification shows zonal pattern of TGF-$\beta$1 cellular stain (inset, 200× magnification). *C,* LFABP-cyclin D1 single transgenic and (*D*) cyclin D1/TGF-$\beta$1 mice at 12 months of age stained with Gomori's trichrome show extensive collagen deposition around portal arteries (*block arrows*) in cyclin D1/TGF-$\beta$1 animals only. Central veins are highlighted by *arrows*.

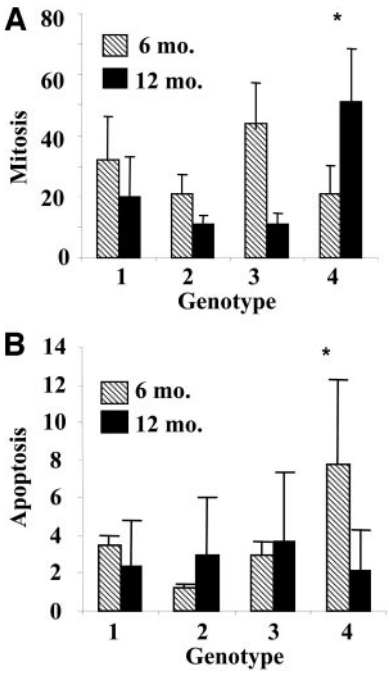


Fig. 2. Dominant effect of Alb-transforming growth factor $\beta$1 (TGF-$\beta$1) transgene on cellular proliferation. *A,* mean counts of KI67-positive hepatocytes (per 10 high-power fields at 400×) for each of $n \geq 4$ mice per group are graphed with SE bars: 1 = wild type, 2 = Alb-TGF-$\beta$1, 3 = LFABP-cyclin D1, and 4 = cyclin D1/TGF-$\beta$1 (*$P < 0.001$ for all combinations). *B,* mean apoptotic bodies counted (per 10 high-power fields at 400×) for $n \geq 4$ mice per group with 1 = wild type, 2 = Alb-TGF-$\beta$1, 3 = LFABP-cyclin D1, and 4 = cyclin D1/TGF-$\beta$1 (*$P < 0.0001$ for all combinations).

A dominant growth-inhibitory effect from elevated levels of mature TGF-$\beta$1 was apparent in hepatocellular proliferation rates by 6 months of age. Thus, although proliferation of hepatocytes from LFABP-cyclin D1 single transgenic mice was elevated more than wild-type mice at 6 months of age, Alb-TGF-$\beta$ and cyclin D1/TGF-$\beta$1 livers exhibited suppressed hepatocellular proliferation (Fig. 2*A*). This pattern was reversed abruptly at the 12-month point. Therefore, there was a marked decrease in mitosis between the 6-month mice and the 12-month mice of all of the types except cyclin D1/TGF-$\beta$1 ($P \leq 0.004$ for each group). There additionally was a significant difference in hepatocellular proliferation between the LFABP-cyclin D1 mice and the cyclin D1/TGF-$\beta$1 mice at 12 months ($P < 0.001$) that was not apparent at 6 months ($P$ = 0.8666).

The increase in hepatocellular proliferation in cyclin D1/TGF-$\beta$1 mice at 12 months of age notably was accompanied by a significant decrease in the rate of hepatocellular apoptosis ($P < 0.0001$ comparing counts of apoptotic bodies at 6 months and 12 months in cyclin D1/TGF-$\beta$1 livers; Fig. 2*B*). These data also revealed a significant increase in apoptosis in the cyclin D1/TGF-$\beta$1 mice compared with control groups at 6 months of age ($P < 0.0001$) but not at 12 months ($P$ = 0.4183). Taken together, this switch from a growth-inhibitory profile at 6 months of age to a growth-promoting profile at 12 months

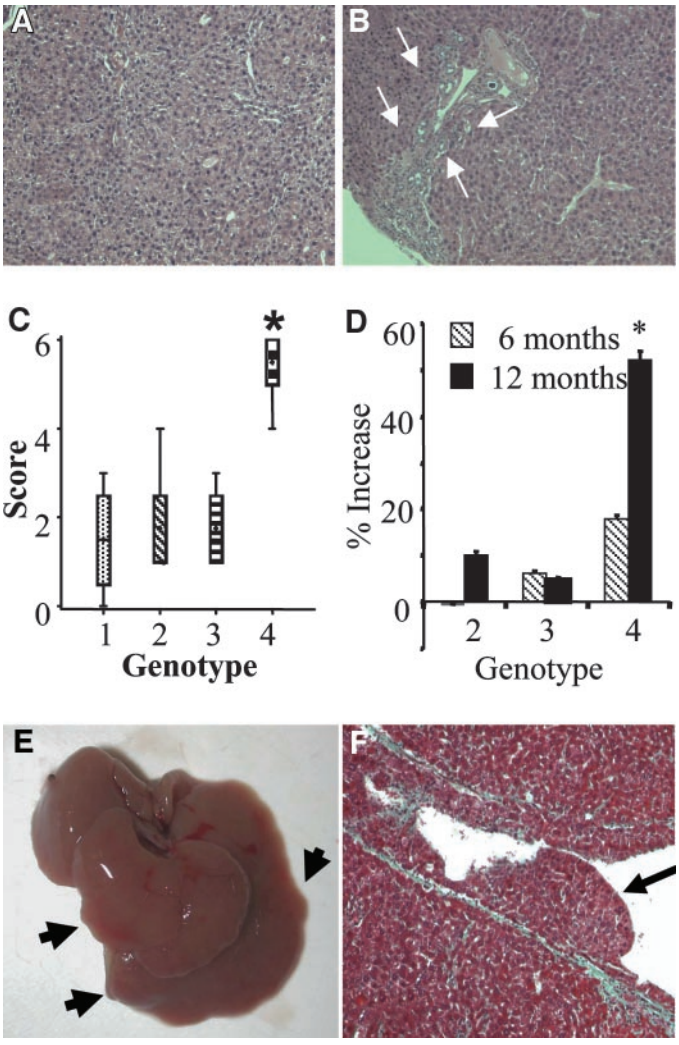


Fig. 3. Hepatic phenotype of cyclin D1/transforming growth factor β1 (TGF-β1) livers. *A*, confluent nodularity: 100× magnification of H&E-stained section of liver from a cyclin D1/TGF-β1 mouse shows pattern of confluent hyperplastic nodularity. *B*, stem cell activation: proliferating lesion of ovoid cells in cholangioles of 12-month-old cyclin D1/TGF-β1 liver is shown at 100× magnification. *C*, precancerous disease: disease progression scores per experimental group at 6 months of age are graphed reflecting cumulative features of early hepatic disease such as nodularity, hyperplasia, and stem cell activation in H&E-stained sections ($n = 4$ for each group): 1 = wild type, 2 = Alb-TGF-β1, 3 = LFABP-cyclin D1, and 4 = cyclin D1/TGF-β1 (*$P < 0.05$ for all combinations). *D*, hepatomegaly: liver weight as a percentage of body weight relative to wild type ($n \geq 4$ each group), 2 = Alb-TGF-β1, 3 = LFABP-cyclin D1, and 4 = cyclin D1/TGF-β1 (*$P < 0.005$ for all combinations). *E*, distorted architecture: cyclin D1/TGF-β1 livers are bulky and nodular at 12 months of age (arrows indicate nodular outgrowths). *F*, hepatocytes that invade central veins: trichrome stain depicts area with marked fibrosis around the central vein and within sinusoids and hepatocellular invasion into the lumen.

of age contrasts dramatically with those of age-matched control hepatocytes.

Accompanying altered cell turnover in cyclin D1/TGF-β1 mice, differences in liver architecture emerged among this group beginning at 6 months of age. As seen in previous studies with LFABP-cyclin D1 mice, zone 3 hepatocytes in cyclin D1/TGF-β1 livers are enlarged and, in many cases, atypical relative to zone 1 and zone 2 hepatocytes. Particular to the cyclin D1/TGF-β1 mice, however, these enlarged cells form foci of confluent bridges involving adjacent lobules suggestive of a chronically regenerative process, and broad areas of compensatory hyperplasia were seen occasionally (Fig. 3*A*). Variability in nuclear size and shape and irregularity of the nuclear membrane are present, and some enlarged cells contain macronuclei. Aberrant, tripolar mitotic figures are seen, as in the LFABP-cyclin D1 line. Hyperchromasia with a coarse chromatin pattern frequently is seen along with nuclear pseudoinclusions. These features, along with the presence of a striking proliferation of small ovoid cells in the region of the terminal bile duct epithelium (cholangioles; Fig. 3*B*), were scored for severity. There is little inflammation associated with proliferative lesion in the cholangioles, and no cholestasis or portal edema is seen. Some portal tracts contain dilated thin-walled blood vessels. The score for architectural nodularity showed significant differences between the cyclin D1/TGF-β1 group and all of the other groups ($P < 0.05$). A summation score, representing the combined score of all of the aforementioned features of hepatic architecture, was determined (Fig. 3*C*). Tests for significance among all of the groups were performed using Tukey adjustment for multiple comparisons (cyclin D1/TGF-β1 *versus* all of the control groups; $P < 0.005$).

By 12 months of age, the liver architecture of cyclin D1/TGF-β1 mice was found to be grossly distorted. Cyclin D1/TGF-β1 livers were significantly bulkier than the control livers (double transgenic *versus* both single transgenic groups, $P < 0.005$; Fig. 3*D*) and exhibited an uneven and nodular profile. The coloration frequently was mottled (Fig. 3*E*). In addition, cyclin D1/TGF-β1 livers contained increased collagen deposition in the sinusoids and surrounding central veins and thickly encompassed all of the vascular and ductal features of the portal triad (Fig. 1*B*). Within these areas, collagen rings, resembling collagen rings found around central veins in Alb-TGF-β1 single transgenic and cyclin D1/TGF-β1 livers, are seen with inclusion of invading hepatocytes sometimes so numerous as to nearly occlude the lumen (Fig. 3*F*). Interestingly, although all of the cyclin D1/TGF-β1 livers showed extensive hepatocellular invasion of central veins (mean, 10 invaded vessels/cm$^2$ by 12 months of age) within and outside visible tumor boundaries, no evidence for distant metastatic spread to lungs, kidneys, or regional lymph nodes was seen.

Frequent expansile nodules of hepatocytes appear in LFABP-cyclin D1 and cyclin D1/TGF-β1 livers beginning at 12 months of age. In contrast with more uniform microscopic lesions originating in LFAB-cyclin D1 livers, early lesions in the cyclin D1/TGF-β1 mice exhibit a markedly varied histology. In addition to basophilic and eosinophilic benign lesions that are typically homogeneous without portal tracts, some lesions appear that exhibit accumulation of lipid within the cellular cytoplasm. Macroscopic tumors could be detected accurately, localized, and characterized by MRI (Fig. 4). Similar to clinical findings with HCC, lesions in these mice exhibit little signal contrast in a T1-weighted MRI (Fig. 4*A*) but show signal hyperintensity in a T2-weighted MRI (Fig. 4*B*). On autopsy, tumor localization, multiplicity, and size are found to correlate reliably with MRI findings, with 89% sensitivity and 70% specificity (data not shown). The overall incidence of HCCs detected by MRI and confirmed at autopsy was higher in cyclin D1/TGF-β1 mice compared with single transgenic mice, whereas the latency of tumor development remained unchanged (Fig. 5*A*). We followed individual animals with tumors by MRI in a series and used a repeated-measures ANOVA, assuming an autoregressive covariance structure, to compare growth rates of tumors detected from 10–15 months of age in LFABP-cyclin D1 mice and cyclin D1/TGF-β1 mice and found there was no significant difference in rate of change ($P = 0.164$) nor in average tumor volume during the period ($P = 0.328$; data not shown). Fifty-three percent of all of the lesions in the LFABP-cyclin D1 mice and 69% of all of the lesions in the cyclin D1/TGF-β1 line at 12 months of age represented HCC or higher-grade tumor. During the lifetime of the mice, the relative risk for carcinoma incidence in the cyclin D1/TGF-β1 mice compared with the LFABP-cyclin D1 mice was 3.89 (95% CI, 1.49, 10.20); the Cochran-Mantel-Haenszel relative risk controlling for age was 3.26 (95% CI, 1.22, 8.69); and the relative risks were homogeneous, with a Breslow-Day test statistic *P* of 0.201. Thus, the cyclin

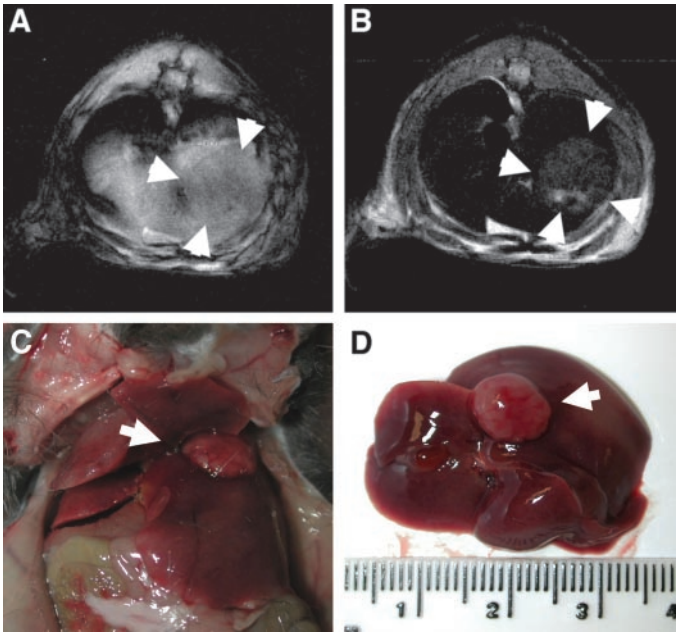


Fig. 4. Hepatocellular carcinoma (HCC) characterization by magnetic resonance imaging (MRI). Representative live-animal 1-mm-thick axial T1-weighted (*A*) and T2-weighted (*B*) MRIs depict a suspected tumor with a 7.5-mm diameter. Matched autopsy photos of HCC *in situ* (*C*) and *ex vivo* (*D*) show 1.6-cm$^3$ tumor with a 7.2-mm diameter on the inferior side of the left lobe.

D1/TGF-$\beta$1 mice were three or four times more likely to develop carcinomas than the LFABP-cyclin D1 mice ($P = 0.004$, when not adjusted for age; $P < 0.03$, when adjusted for age). In addition to higher tumor incidence, age-matched cyclin D1/TGF-$\beta$1 mice exhibited a higher tumor multiplicity compared with LFABP-cyclin D1 single transgenic mice ($P < 0.04$; Fig. 5*B*). There were no measurable differences between LFABP-cyclin D1 and cyclin D1/TGF-$\beta$1 calculated average lesion diameter as tumors progressed (data not shown). Therefore, significant increases in overall tumor burden, as measured by the volume of liver taken up by tumor, were higher in cyclin D1/TGF-$\beta$1 animals compared with age-matched wild-type and single transgenic controls.

We used protein lysates derived from tumor and nontumor tissue from control and experimental groups to test for molecular indicators of the growth-inhibitory (Smad-dependent) pathway of TGF-$\beta$ signaling. The striking finding from these experiments is that a proportion of mice from each transgenic group, but no animals from the wild-type group, exhibited a loss of Smad4 expression in their livers beginning at 6 months of age (Fig. 6; Table 1). Smad2/3:Smad4 complex formation among Smad4-positive tissues was similar statistically in all of the groups tested. When protein lysates from isolated tumors *versus* adjacent uninvolved tissue were compared, there was no significant difference in Smad4 expression for either transgenic group ($P = 0.335$).

A small group of animals ($n \geq 4$ each for LFABP-cyclin D1 and cyclin D1/TGF-$\beta$1 group) was followed to 17 months of age. Heterogeneous signal enhancement of tumor in the T2-weighted images, clinically characteristic of malignant lesions, was seen in a subset of cyclin D1/TGF-$\beta$1 livers only (Fig. 7*A*). The internally heterogeneous lesions often were associated with large tumors that appeared to engulf the entire organ and had indistinct margins on autopsy. Histopathology of these large lesions revealed tumors of mixed cellular differentiation, including extensive endothelial cell proliferation. For one lesion in particular, the heterogeneous MRI pattern was associated with a lesion whose features were consistent with angiosarcoma. Irregularly formed blood vessels along sinusoids in this area of interest stained strongly for the endothelial marker CD31 (Fig. 7*B*).

## DISCUSSION

We followed the natural fate of tumor progression in LFABP-cyclin D1 transgenic mice in the context of prolonged TGF-$\beta$1 expression in mice that harbor cyclin D1 and TGF-$\beta$1 hepatocyte-specific transgenes. We introduced the use of MRI to follow these animals over time and to characterize the primary and secondary hepatic lesions. This imaging aspect of the study is important for several reasons, most notably for the application of noninvasive clinical methods to an experimental mouse model. The approach of noninvasive imaging

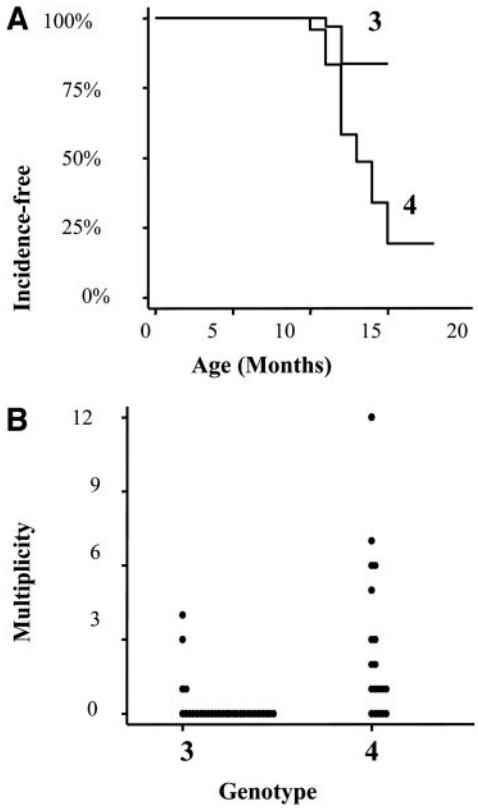


Fig. 5. Cyclin D1/transforming growth factor $\beta$1 (TGF-$\beta$1) mice have increased tumor incidence and tumor multiplicity. *A*, the hepatocellular carcinoma incidence-free proportions of LFABP-cyclin D1 (*3*) and cyclin D1/TGF-$\beta$1 (*4*; $n \geq 12$ for each group). *B*, numbers of individual macroscopic tumors counted per age-matched liver at 13 months of age in individual LFABP-cyclin D1 (*3*) *versus* cyclin D1/TGF-$\beta$1 (*4*) mice ($P = 0.0003$).

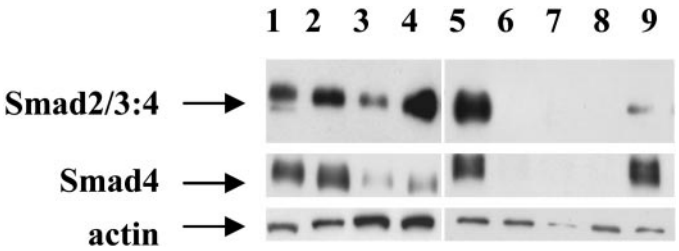


Fig. 6. Transgenic liver tissues down-regulate Smad4 expression. Representative Smad4 immunoblots of protein lysates from control and experimental mouse livers are shown. Animals were scored positive (+) or negative (−) for Smad4 expression and Smad2/3:Smad4 complex formation: 1 = wild-type liver, 2 = LFABP-cyclin D1 liver, 3 = cyclin D1/transforming growth factor $\beta$1 (TGF-$\beta$1) liver/no tumor, 4 = cyclin D1/TGF-$\beta$1 tumor tissue, 5 = cyclin D1/TGF-$\beta$1 tissue/no tumor, 6 = cyclin D1/TGF-$\beta$1 tumor tissue, 7 = cyclin D1/TGF-$\beta$1 tissue/no tumor, 8 = cyclin D1/TGF-$\beta$1 tumor tissue, and 9 = cyclin D1/TGF-$\beta$1 tissue/no tumor.

Table 1 *Transgenic mouse livers exhibit loss of Smad4 expression*

The proportion of animals in each group with a positive score for Smad4 expression and for Smad2/3:4 complex formation ($n \geq 10$ each group) is given with 95% confidence intervals in parenthesis.

| | Smad4 | Smad2/3:4 complex |
|---|---|---|
| Wild type | 100% (100–100%) | 45% (18–72%) |
| Alb-TGF-β[a] | 55% (27–83%) | n.d.[a] |
| LFABP-cyclin D1 | 46% (19–73%) | 26% (−1.2–53%) |
| Double transgenic | 41% (18–64%) | 31% (9–53%) |

[a] TGF-β, transforming growth factor β; n.d., not done.

also has potential for a significant reduction in the number of animals used in a longitudinal study.

The degree of Alb-TGF-β1 transgene expression in control and experimental mice is consistent with the well-characterized pattern of expression described elsewhere (24). Some endogenous TGF-β1 production was observed at late time points (>6 months) in LFABP-cyclin D1 control mice. Immunostaining for TGF-β1 in LFABP-cyclin D1 livers indicates that the pericentral dysplastic hepatocytes are the primary source of the endogenous TGF-β1 (Fig. 1*A*). Expression of endogenous TGF-β1 in single transgenic control mice may be a consequence of a negative regulatory mechanism in response to increased hepatocellular proliferation in this line. Similar increases in TGF-β expression have been described previously during hepatic regeneration following 70% hepatectomy (32). Immunostaining of cyclin D1/TGF-β1 livers demonstrates that TGF-β1 activity accumulates to higher levels in cyclin D1/TGF-β1 livers than in LFABP-cyclin D1 livers (Fig. 1*B*) and that its expression is not restricted to pericentral hepatocytes. Total levels of circulating TGF-β1 also are increased 2.5–3.7-fold in cyclin D1/TGF-β1 mice *versus* each of the single transgenic controls, suggesting an additive effect. Evidence for the abundant presence of the mature, active form of TGF-β1 in the circulation of experimental cyclin D1/TGF-β1 mice includes the presence of the global diffuse kidney disease in Alb-TGF-β1 and cyclin D1/TGF-β1 mice but not in wild-type or LFABP-cyclin D1 mice and the presence of pervasive hepatic fibrosis in the Alb-TGF-β1 and cyclin D1/TGF-β1 mice but not in the LFABP-cyclin D1 mice (Fig. 1, *C* and *D*). In conclusion, up-regulation of endogenous latent TGF-β1 by aberrantly cycling hepatocytes is insufficient to cause the enhanced tumor phenotype seen in the cyclin D1/TGF-β1 mice, but rather the prolonged effect of high levels of the active form of TGF-β1 was responsible for the higher incidence and the development of more numerous and more aggressive lesions seen in experimental cyclin D1/TGF-β1 livers.

We found that overexpression of mature TGF-β1 had an early growth-inhibitory effect on LFABP-cyclin D1 hepatocytes that was overcome subsequently by a failure of cells to respond to TGF-β by apoptosis at 12 months of age. The overexpression of TGF-β1 alone in Alb-TGF-β1 mice is accompanied by increased hepatocellular apoptosis (24). Growth inhibition by mature TGF-β1 is known to block quiescent hepatocytes from replication and to prepare them for apoptosis *in vitro* and *in vivo* (16). This apoptotic response is consistent with the role of TGF-β in hepatocellular cultures and regressing livers (33, 34). Similar phenomena have linked the activation of Smad-pathway inhibitors, namely Smad7, with the triggering of epithelial cell apoptosis (35–37). Several lines of evidence also show that TGF-β-mediated apoptosis is linked to activation of TGF type II receptor and Smad signaling (38–40). Inactivation of the growth-inhibitory, or Smad, pathway of TGF-β signal transduction has been shown to be an important mechanism in the development of a variety of human cancers and may be related to the loss of the apoptotic response (41, 42).

Interestingly, transient inhibition of the Smad-dependent TGF-β signal transduction pathway has been observed in disease-associated physiologic processes in the liver, such as with compensatory liver hyperplasia following acute liver injury. Furthermore, it is known that replicating hepatocytes exhibit a transitory insensitivity to TGF-β following partial hepatectomy (43). Whereas Smad4 expression was lost in a percentage of LFABP-cyclin D1 and cyclin D1/TGF-β1 livers (Table 1), the loss of apoptotic response to TGF-β at 12 months of age was unique to cyclin D1/TGF-β1 livers (Fig. 2*B*), suggesting that this phenomenon was not directly a consequence of changes in Smad-dependent signaling. Because the apoptotic response was not as high at 6 months in either of the single transgenic control groups as in the double transgenic group, these data suggest that cells did not experience the same degree of selective pressure for TGF-β resistance as in the D1/TGF-β1 livers, either because the TGF-β was not activated (in the case of the LFABP-cyclin D1 group) or because there was no cyclin D1 overexpression (in the case of the Alb-TGF-β1 group). Thus, the added selective pressure in the D1/TGF-β1 livers is likely causal for the increased tumor incidence and tumor burden in this group.

The observation made on growth inhibition of hepatocytes in these animals particularly is of interest when considered with the appearance of a consistent expansion of the cellular compartment resembling and emanating from the area of the peripheral bile ducts (Fig. 3*B*). The lesions discovered in the cyclin D1/TGF-β1 livers resemble ductal plate malformations of the small capillary ductules of the periphery known as von Meyenburg complexes in humans, also commonly referred to as interlobular bile ducts, and may represent activation of the hepatic stem cell compartment (44). Ductal plate malformation is seen to a slight degree in Alb-TGF-β1 livers but is more pronounced in the cyclin D1/TGF-β1 livers. Previous experiments suggest that the developmental timing of TGF-β1 exposure to hepatic stem cell populations predetermines proliferation in this putative stem cell compartment (44, 45). Hepatic stem cells may be thought of as a "facultative" stem cell compartment because they are activated only under defined circumstances (46). Whereas the first line of defense to liver injury is regeneration by replication of fully differentiated hepatocytes and biliary epithelial cells themselves, it now is recognized that the replicative capacity of the fully differentiated epithelial cells must be compromised for the stem cell compartment to become activated (47, 48). Activation of stem cells results in proliferation of small cells with little cytoplasm, called "oval" cells, around the periductal space. This phenomenon produces a series of irregular ductal structures that

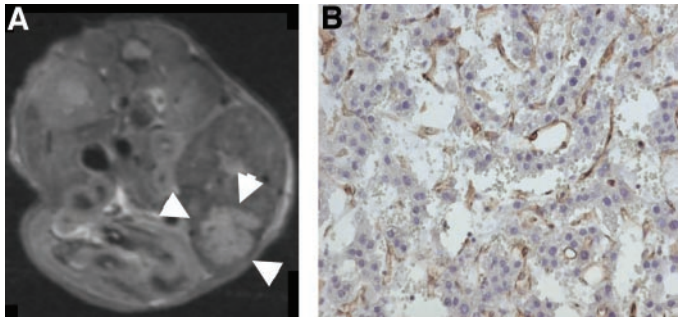


Fig. 7. Cyclin D1/transforming growth factor β1 (TGF-β1) tumors are heterogeneous and aggressive in their phenotype. *A*, T2-weighted magnetic resonance image of tumor from cyclin D1/TGF-β1 transgenic mouse shows area of marked hyperintensity (*arrows*) within the boundary of a tumor. *B*, 200× magnification of CD31-stained section from tumor imaged in (*A*) shows irregular vascular channels and dilated sinusoids lined with endothelial cells (*stained brown*).

remain connected to bile ducts, similar to those that appear in the cyclin D1/TGF-$\beta$1 livers. In conclusion, the particular growth-inhibitory effect of the TGF-$\beta$1 transgene resulted in a replicative exhaustion or compromise of the differentiated epithelial cell compartment and a subsequent activation of the stem cell compartment in cyclin D1/TGF-$\beta$1 livers.

A significant increase in the incidence and multiplicity of liver nodules in cyclin D1/TGF-$\beta$1 mice compared with LFABP-cyclin D1 mice confirms previous data showing that TGF-$\beta$1 acts as a tumor promoter *in vivo* (49). However, a novel and striking difference in tumors between the control and experimental livers in this experiment was in the characterization of hepatocellular features seen in transgenic livers and in the tumors themselves. Thus, although LFABP-cyclin D1 single transgenic mice developed relatively homogeneous tumors and the hepatocytes generally were "well behaved," the cyclin D1/TGF-$\beta$1 mice developed lesions of a mixed cell type, including hepatocellular, endothelial, and ductal epithelial forms, and strikingly, hepatocytes from all of the cyclin D1/TGF-$\beta$1 mice routinely were found invading the vascular wall of central veins (Fig. 4*F*). This fascinating hallmark of D1/TGF-$\beta$1 livers demonstrates enhanced migratory capacity in these cells. Interestingly, autocrine TGF-$\beta$ signaling at low thresholds likewise has been demonstrated to enhance tumor cell motility and invasiveness through deposits of extracellular matrix *in vitro* (13, 17, 50).

Clinically, primary tumors of the liver with a malignant phenotype have characteristic MRI signal intensity profiles that include hyperintensity on a T2-weighted image (25). This characteristic was consistent with heterogeneous enhanced signal intensity in T2-weighted images of high-grade tumors in cyclin D1/TGF-$\beta$1 livers (Fig. 7*A*). Hepatic peliosis (angiosarcoma), consisting of broad areas of sinusoidal dilation and hemorrhagic cysts with irregular vascular channels invading the adjacent parenchyma, was associated with the heterogeneous T2-weighted pattern noted in an individual mouse among the cyclin D1/TGF-$\beta$1 group. These features are consistent with activity of the paracrine tumor-promoting effects on the recruitment of endothelial cells and the promotion of angiogenesis (51–53).

In summary, the tumor-promoting effects of TGF-$\beta$1 predominated over the growth-inhibitory effects in this model of HCC progression and brought about a higher incidence of tumors with a more aggressive phenotype. The use of MRI to characterize tumor development was useful to reduce the study sample size and also to characterize tumor growth rate and malignancy. The assessment of accuracy of MRI detection and serial imaging of primary liver tumors using high field magnets specifically designed for small animal imaging is underway[8] and should prove to be valuable to adapt this model to test additional mechanisms of tumor progression and therapeutic strategies, including those that exploit molecular targets such as cyclin D1 and TGF-$\beta$.

## ACKNOWLEDGMENTS

We thank the Vanderbilt University Small Animal Pathology and Histopathology Core Laboratory, run by Lillian B. Nanney and Kelly Parman, and the Division of Animal Care, directed by Joan Richerson and Greg Hanley, for their contributions. We also thank Dr. Ron Arildsen of the VUMC Department of Radiology for his critical review of this manuscript.

## REFERENCES

1. Tanaka, Y., Hanada, K., Mizokami, M., Yeo, A. E., Shih, J. W., Gojobori, T., and Alter, H. J. Inaugural article: a comparison of the molecular clock of hepatitis C virus in the United States and Japan predicts that hepatocellular carcinoma incidence in the United States will increase over the next two decades. Proc. Natl. Acad. Sci. USA, *99:* 15584–15589, 2002.
2. El-Serag, H. B., and Mason, A. C. Rising incidence of hepatocellular carcinoma in the United States. N. Engl. J. Med., *340:* 745–750, 1999.
3. Thorgeirsson, S. S., and Grisham, J. W. Molecular pathogenesis of human hepatocellular carcinoma. Nat. Genet., *31:* 339–346, 2002.
4. Zhang, Y. J., Jiang, W., Chen, C. J., Lee, C. S., Kahn, S. M., Santella, R. M., and Weinstein, I. B. Amplification and overexpression of cyclin D1 in human hepatocellular carcinoma. Biochem. Biophys. Res. Commun., *196:* 1010–1016, 1993.
5. Masaki, T., Shiratori, Y., Rengifo, W., Igarashi, K., Yamagata, M., Kurokohchi, K., Uchida, N., Miyauchi, Y., Yoshiji, H., Watanabe, S., Omata, M., and Kuriyama, S. Cyclins and cyclin-dependent kinases: comparative study of hepatocellular carcinoma versus cirrhosis. Hepatology, *37:* 534–543, 2003.
6. Hall, M., and Peters, G. Genetic alterations of cyclins, cyclin-dependent kinases, and Cdk inhibitors in human cancer. Adv. Cancer Res., *68:* 67–108, 1996.
7. Taub, R. Expression and function of growth-induced genes during liver regeneration. *In:* R. L. Jirtle (ed.), Liver Regeneration and Carcinogenesis: Molecular and Cellular Mechanisms. San Diego: Academic Press, 1995.
8. Jiang, W., Kahn, S. M., Zhou, P., Zhang, Y. J., Cacace, A. M., Infante, A. S., Doi, S., Santella, R. M., and Weinstein, I. B. Overexpression of cyclin D1 in rat fibroblasts causes abnormalities in growth control, cell cycle progression and gene expression. Oncogene, *8:* 3447–3457, 1993.
9. Quelle, D. E., Ashmun, R. A., Shurtleff, S. A., Kato, J. Y., Bar-Sagi, D., Roussel, M. F., and Sherr, C. J. Overexpression of mouse D-type cyclins accelerates G1 phase in rodent fibroblasts. Genes Dev., *7:* 1559–1571, 1993.
10. Resnitzky, D., Gossen, M., Bujard, H., and Reed, S. I. Acceleration of the G1/S phase transition by expression of cyclins D1 and E with an inducible system. Mol. Cell. Biol., *14:* 1669–1679, 1994.
11. Deane, N. G., Parker, M. A., Aramandla, R., Diehl, L., Lee, W. J., Washington, M. K., Nanney, L. B., Shyr, Y., and Beauchamp, R. D. Hepatocellular carcinoma results from chronic cyclin D1 overexpression in transgenic mice. Cancer Res., *61:* 5389–5395, 2001.
12. DuBois, R. N., Myers, D., and Beauchamp, R. D. Growth inhibitory signals and liver regeneration: the TGFβ superfamily. *In:* A. M. Diehl (ed.), Liver Growth and Repair. London: Chapman and Hall, 1998.
13. Derynck, R., Akhurst, R. J., and Balmain, A. TGF-$\beta$ signaling in tumor suppression and cancer progression. Nat. Genet., *29:* 117–129, 2001.
14. Roberts, A. B., Thompson, N. L., Heine, U., Flanders, C., and Sporn, M. B. Transforming growth factor-$\beta$: possible roles in carcinogenesis. Br. J. Cancer, *57:* 594–600, 1988.
15. Ko, T. C., Sheng, H. M., Reisman, D., Thompson, E. A., and Beauchamp, R. D. Transforming growth factor-$\beta$ 1 inhibits cyclin D1 expression in intestinal epithelial cells. Oncogene, *10:* 177–184, 1995.
16. Santoni-Rugiu, E. and Thorgeirsson, S. S. Transgenic animals as models for hepatocarcinogenesis. *In:* A. M. Diehl (ed.), Liver Growth and Repair, pp. 100–142. London: Chapman and Hall, 1998.
17. Dumont, N., and Arteaga, C. L. Transforming growth factor-$\beta$ and breast cancer: tumor promoting effects of transforming growth factor-$\beta$. Breast Cancer Res., *2:* 125–132, 2000.
18. Fowlis, D. J., Cui, W., Johnson, S. A., Balmain, A., and Akhurst, R. J. Altered epidermal cell growth control *in vivo* by inducible expression of transforming growth factor $\beta$1 in the skin of transgenic mice. Cell Growth Differ., *7:* 679–687, 1996.
19. Ito, N., Kawata, S., Tamura, S., Takaishi, K., Shirai, Y., Kiso, S., Yabuuchi, I., Matsuda, Y., Nishioka, M., and Tarui, S. Elevated levels of transforming growth factor $\beta$ messenger RNA and its polypeptide in human hepatocellular carcinoma. Cancer Res., *51:* 4080–4083, 1991.
20. Shirai, Y., Kawata, S., Ito, N., Tamura, S., Takaishi, K., Kiso, S., Tsushima, H., and Matsuzawa, Y. Elevated levels of plasma transforming growth factor-$\beta$ in patients with hepatocellular carcinoma. Jpn. J. Cancer Res., *83:* 676–679, 1992.
21. Pierce, D. F., Jr., Johnson, M. D., Matsui, Y., Robinson, S. D., Gold, L. I., Purchio, A. F., Daniel, C. W., Hogan, B. L., and Moses, H. L. Inhibition of mammary duct development but not alveolar outgrowth during pregnancy in transgenic mice expressing active TGF-$\beta$1. Genes Dev., *7:* 2308–2317, 1993.
22. Pierce, D. F., Jr., Gorska, A. E., Chytil, A., Meise, K. S., Page, D. L., Coffey, R. J., Jr., and Moses, H. L. Mammary tumor suppression by transforming growth factor $\beta$ 1 transgene expression. Proc. Natl. Acad. Sci. USA, *92:* 4254–4258, 1995.
23. Jhappan, C., Geiser, A. G., Kordon, E. C., Bagheri, D., Hennighausen, L., Roberts, A. B., Smith, G. H., and Merlino, G. Targeting expression of a transforming growth factor $\beta$1 transgene to the pregnant mammary gland inhibits alveolar development and lactation. EMBO J., *12:* 1835–1845, 1993.
24. Sanderson, N., Factor, V., Nagy, P., Kopp, J., Kondaiah, P., Wakefield, L., Roberts, A. B., Sporn, M. B., and Thorgeirsson, S. S. Hepatic expression of mature transforming growth factor $\beta$1 in transgenic mice results in multiple tissue lesions. Proc. Natl. Acad. Sci. USA, *92:* 2572–2576, 1995.
25. Coakley, F. V., and Schwartz, L. H. Imaging of hepatocellular carcinoma: a practical approach. Semin. Oncol., *28:* 460–473, 2001.
26. Teefey, S. A., Hildeboldt, C. C., Dehdashti, F., Siegel, B. A., Peters, M. G., Heiken, J. P., Brown, J. J., McFarland, E. G., Middleton, W. D., Balfe, D. M., and Ritter, J. H. Detection of primary hepatic malignancy in liver transplant candidates: prospective comparison of CT, MR imaging, US, and PET. Radiology, *226:* 533–542, 2003.
27. Rummeny, E., Weissleder, R., Stark, D. D., Saini, S., Compton, C. C., Bennett, W., Hahn, P. F., Wittenberg, J., Malt, R. A., and Ferrucci, J. T. Primary liver tumors: diagnosis by MR imaging. AJR Am. J. Roentgenol., *152:* 63–72, 1989.
28. Hussain, S. M., Semelka, R. C., and Mitchell, D. G. MR imaging of hepatocellular carcinoma. Magn. Reson. Imaging Clin. N. Am., *10:* 31–52, 2002.

[8] Unpublished observations.

29. Hussain, S. M., Zondervan, P. E., IJzermans, J. N., Schalm, S. W., de Man, R. A., and Krestin, G. P. Benign versus malignant hepatic nodules: MR imaging findings with pathologic correlation. Radiographics, *22:* 1023–1036; discussion 1037–1029, 2002.
30. Saha, D., Datta, P. K., and Beauchamp, R. D. Oncogenic ras represses transforming growth factor-β/Smad signaling by degrading tumor suppressor Smad4. J. Biol. Chem., *276:* 29531–29537, 2001.
31. Kopp, J. B., Factor, V. M., Mozes, M., Nagy, P., Sanderson, N., Bottinger, E. P., Klotman, P. E., and Thorgeirsson, S. S. Transgenic mice with increased plasma levels of TGF-β1 develop progressive renal disease. Lab. Invest., *74:* 991–1003, 1996.
32. Bissell, D., Wang, S., Jarnagin, W., and Roll, F. Cell specific expression of transforming growth factor β in rat liver. Evidence for autocrine regulation of hepatocyte proliferation. J. Clin. Investig., *96:* 447–455, 1995.
33. Oberhammer, F. A., Pavelka, M., Sharma, S., Tiefenbacher, R., Purchio, A. F., Bursch, W., and Schulte-Hermann, R. Induction of apoptosis in cultured hepatocytes and in regressing liver by transforming growth factor β1. Proc. Natl. Acad. Sci. USA, *89:* 5408–5412, 1992.
34. Oberhammer, F., Bursch, W., Tiefenbacher, R., Froschl, G., Pavelka, M., Purchio, T., and Schulte-Hermann, R. Apoptosis is induced by transforming growth factor-β1 within 5 hours in regressing liver without significant fragmentation of the DNA. Hepatology, *18:* 1238–1246, 1993.
35. Lallemand, F., Mazars, A., Prunier, C., Bertrand, F., Kornprost, M., Gallea, S., Roman-Roman, S., Cherqui, G., and Atfi, A. Smad7 inhibits the survival nuclear factor κB and potentiates apoptosis in epithelial cells. Oncogene, *20:* 879–884, 2001.
36. Yang, Y. A., Tang, B., Robinson, G., Hennighausen, L., Brodie, S. G., Deng, C. X., and Wakefield, L. M. Smad3 in the mammary epithelium has a nonredundant role in the induction of apoptosis, but not in the regulation of proliferation or differentiation by transforming growth factor-β. Cell Growth Differ., *13:* 123–130, 2002.
37. Schuster, N., and Krieglstein, K. Mechanisms of TGF-β-mediated apoptosis. Cell Tissue Res., *307:* 1–14, 2002.
38. Wildey, G. M., Patil, S., and Howe, P. H. Smad3 potentiates transforming growth factor β-induced apoptosis and expression of the BH3-only protein Bim in WEHI 231 B lymphocytes. J. Biol. Chem., *278:* 18069–18077, 2003.
39. Edlund, S., Bu, S., Schuster, N., Aspenstrom, P., Heuchel, R., Heldin, N. E., Ten Dijke, P., Heldin, C. H., and Landstrom, M. Transforming growth factor-β1 (TGF-β)-induced apoptosis of prostate cancer cells involves Smad7-dependent activation of p38 by TGF-β-activated kinase 1 and mitogen-activated protein kinase kinase 3. Mol. Biol. Cell, *14:* 529–544, 2003.
40. Itoh, S., Thorikay, M., Kowanetz, M., Moustakas, A., Itoh, F., Heldin, C. H., and ten Dijke, P. Elucidation of Smad requirement in transforming growth factor-β type I receptor-induced responses. J. Biol. Chem., *278:* 3751–3761, 2003.
41. Hata, A., Shi, Y., and Massague, J. TGF-β signaling and cancer: structural and functional consequences of mutations in Smads. Mol. Med. Today, *4:* 257–262, 1998.
42. Kim, S. J., Im, Y. H., Markowitz, S. D., and Bang, Y. J. Molecular mechanisms of inactivation of TGF-β receptors during carcinogenesis. Cytokine Growth Factor Rev., *11:* 159–168, 2000.
43. Russell, W. E., Coffey, R. J., Jr., Ouellette, A. J., and Moses, H. L. Type β transforming growth factor reversibly inhibits the early proliferative response to partial hepatectomy in the rat. Proc. Natl. Acad. Sci. USA, *85:* 5126–5130, 1988.
44. Desmet, V. J. Ludwig symposium on biliary disorders—part I. Pathogenesis of ductal plate abnormalities. Mayo. Clin. Proc., *73:* 80–89, 1998.
45. Desmet, V. J. Congenital diseases of intrahepatic bile ducts: variations on the theme "ductal plate malformation." Hepatology, *16:* 1069–1083, 1992.
46. Thorgeirsson, S. S. Stem cells and hepatocarcinogenesis. *In:* R. L. Jirtle (ed.), Liver Regeneration and Carcinogenesis, Molecular and Cellular Mechanisms, pp. 99–112. San Diego: Academic Press, 1995.
47. Grisham, J. W. Cell types in long-term propagable cultures of rat liver. Ann. N. Y. Acad. Sci., *349:* 128, 1980.
48. Dabeva, M. D., and Shafritz, D. A. Activation, proliferation, and differentiation of progenitor cells into hepatocytes in the D-galactosamie model of liver regeneration. Am. J. Pathol., *143:* 1606–1620, 1993.
49. Factor, V. M., Kao, C. Y., Santoni-Rugiu, E., Woitach, J. T., Jensen, M. R., and Thorgeirsson, S. S. Constitutive expression of mature transforming growth factor β1 in the liver accelerates hepatocarcinogenesis in transgenic mice. Cancer Res., *57:* 2089–2095, 1997.
50. Dumont, N., Bakin, A. V., and Arteaga, C. L. Autocrine transforming growth factor-β signaling mediates Smad-independent motility in human cancer cells. J. Biol. Chem., *278:* 3275–3285, 2003.
51. Tuxhorn, J. A., McAlhany, S. J., Yang, F., Dang, T. D., and Rowley, D. R. Inhibition of transforming growth factor-β activity decreases angiogenesis in a human prostate cancer-reactive stroma xenograft model. Cancer Res., *62:* 6021–6025, 2002.
52. Breier, G., Blum, S., Peli, J., Groot, M., Wild, C., Risau, W., and Reichmann, E. Transforming growth factor-β and Ras regulate the VEGF/VEGF-receptor system during tumor angiogenesis. Int. J. Cancer, *97:* 142–148, 2002.
53. Kuzuya, M., and Kinsella, J. L. Reorganization of endothelial cord-like structures on basement membrane complex (Matrigel): involvement of transforming growth factor β1. J. Cell Physiol., *161:* 267–276, 1994.